Enhanced adaptive subtraction method for simultaneous source separation

Zhaojun Liu, Bin Wang, Jim Specht, Jeffery Sposato and Yongbo Zhai, TGS*

Summary

We have developed an iterative adaptive subtraction method to separate shot blended data. The model of coherent events is determined and alternately adaptively subtracted from the primary and secondary sets of shot data in their respective common offset gathers. We add the residual from a given iteration to the other set of shot data for the next iteration. This iterative process reconstructs the deblended data of both sets of shots simultaneously. We illustrate our method by generating simulated simultaneous source data using the synthetic Marmousi data. The results show little crosstalk remaining after deblending and the migration images are very similar to those of the unblended data.

Introduction

In recent years, more and more oil and service companies have studied simultaneous shooting for marine acquisition. Compared to conventional marine seismic acquisition, simultaneous shooting can either reduce the acquisition costs by reducing the temporal shot intervals, or increase the shot density in the same acquisition time. Furthermore, it can also gain both benefits by combining the two approaches.

The processing of the simultaneous source data can be similar to conventionally acquired data but it introduces crosstalk artifacts to the migration image from incongruous sources and thus decreases the imaging quality. Many different data separation techniques exist to separate the data and minimize the interference between sources. These approaches separate into two main categories: passive separation and active separation.

Active separation methods solve the data deblending as an inversion problem (Moore et al., 2008; Abma et al., 2010). We transform the simultaneous source data to a sparse model domain so the events from different shots are better separated and thus help to reconstruct the deblended data.

Passive approaches usually start from the pseudodeblended data and sort the result into another domain where the blending noise becomes incoherent. These approaches remove the noise either by coherency filters (Beasley et al., 1998, Huo et al., 2012), or by iterative subtraction (Mahdad et al., 2011, Peng et al., 2013).

TGS developed adaptive subtraction flows to separate simultaneous sources for OBC data (Kim et al, 2009). It is very effective in attenuating the interference in the data while preserving the weak signal, but the drawback is the separation failed when the distance of the simultaneous shots is small so that the interferences are the same amplitude level as the coherent signal. The simulation tests show shot distance should be greater than 2 km.

Here we improve on this method by subtracting the incoherent noise and adding the residual back to the data in an iterative approach. We demonstrate that the enhanced method can separate the blended data with weak events preserved and very little leakage, even with adjacent simultaneous sources. We know that the interference from adjacent shots mainly affect the shallow part of migration image while the interference from a blended distant source may damage the deeper structural events.

Enhanced Adaptive Subtraction Flow

Figure 1 shows the adaptive subtraction flow (Kim et al., 2009). We refer to “primary” as those shots fired on a predetermined firing cycle and refer to “secondary” as the shots fired with a random delay (or in advance, with respect to the primary shots). By shifting the shot records, we can make the primary shot response coherent and secondary shot responses random, and vice versa, and we call them primary shot domain data and secondary shot domain data respectively.

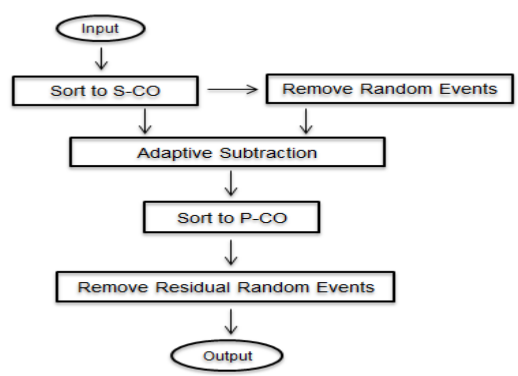

Figure 1: Flow diagram for adaptive subtraction to separate simultaneous sources and recover the primary shots. S-CO is Secondary Common Offset Ensembles and P-CO is Primary Common Offset Ensembles (Kim et al., 2009)

To ensure the model for adaptive subtraction of the secondary shot does not include any primary events, we apply a somewhat harsh filter to the data that distorts the secondary events in the model. Even adaptive subtraction cannot compensate for all the differences so secondary shot

DOI http://dx.doi.org/10.1190/segam2014-1510.1

residual energy remains after subtraction. The final step of applying a median filter may attenuate some of the residual energy but also may damage the primary shot events. This problem can magnify, especially in the case where the simultaneous source distance is small. We developed an enhanced adaptive subtraction flow to remove the interference and reconstruct both primary and secondary shot data simultaneously by iteration.
Figure 2 shows the modified job flow for the adaptive subtraction part. Instead of median filtering at the final

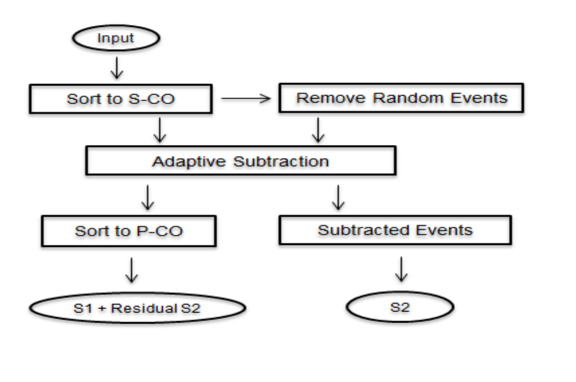

Figure 2: Revised adaptive subtraction flow: Instead of median filtering at the final step, the data is separated by two parts: the part after adaptive subtraction includes all of the primary shot events and leakage from secondary shots, whereas the part containing the subtracted events includes mostly secondary shot events only.

step, we separate the data into two parts after adaptive subtraction. The part that remains after subtraction includes all of the primary shot events and some leakage from secondary shots. The subtracted part includes events from secondary shots only if we applied a sufficiently aggressive filter to generate the subtraction model. Note this processing procedure also separates coherent event and random noise in primary shot common offset domain, so we can repeat it by subtraction and addition alternately to reconstruct both the primary and secondary source events simultaneously by iteration, as shown in Figure 3.

The initial processing step is in the secondary shot domain. We can select a very aggressive median filter to build up the model for the secondary shot coherent events. Therefore, after the first iteration, the reconstructed primary shot data contains almost all the primary shot events and some leakage from secondary shots, while the reconstructed secondary data contains only secondary shot events with distortion.

The next processing step is in the primary shot domain. The reconstructed primary data in the previous step separates into two parts. One is the reconstructed primary shot data with less distortion, and we add the other part to the reconstructed secondary shot data in the previous step to make new reconstructed secondary shot data.
We repeat the above steps in primary shot and secondary shot common offset domain alternately. After a few

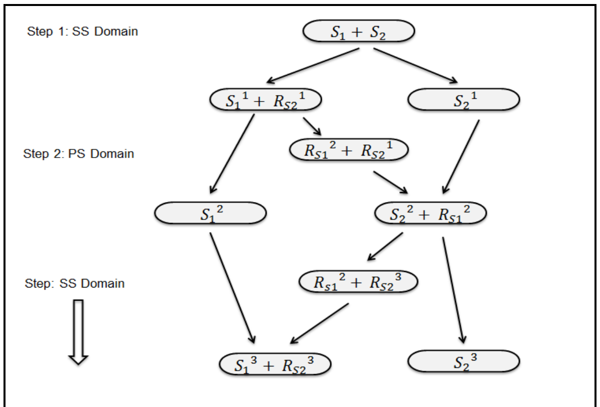

Figure 3: Iterative processing flow for enhanced adaptive subtraction approach. PS is Primary Shot Domain and SS is Secondary Shot Domain. The subscripts represent the source index and the superscripts represent the number of iteration.

iterations, we reconstruct both primary shot and secondary shot data simultaneously. The cross-shot leakage is insignificant compared to the signal. We will show the results with simulated synthetic data tests.

Deblending Results

We tested this approach on 2D synthetic streamer data. We used the Marmousi model to generate the synthetic data set, which contains complex structures, steeply dipping diffractions, and weak coherent events in order to demonstrate the effectiveness of our approach on different cases. The receiver spacing is 12.5 m. The source interval for both primary and secondary shots is 25 m, and the offset between primary shot and secondary shots is 12.5 m. The time delay of the secondary shot to the primary shot is a random dithering time within the range of 100 ms to 600 ms. The previous adaptive subtraction method (Kim, 2009) is not robust in separating adjacent simultaneous shot data, so it is not here for comparison. We present the reconstructed results from blended data.

Figures 4a-4h show the common offset gathers of following: (a) blended primary source, (b) reconstructed primary source, (c) the true unblended primary source,(d) difference between reconstructed and unblended primary source, (e) blended secondary source, (f) reconstructed secondary source, (g) the true unblended secondary source, and (h) difference between reconstructed and unblended secondary source. Figures 4i-4p show the corresponding data in a zoomed-in area that is marked in Figure 4a.

DOI http://dx.doi.org/10.1190/segam2014-1510.1

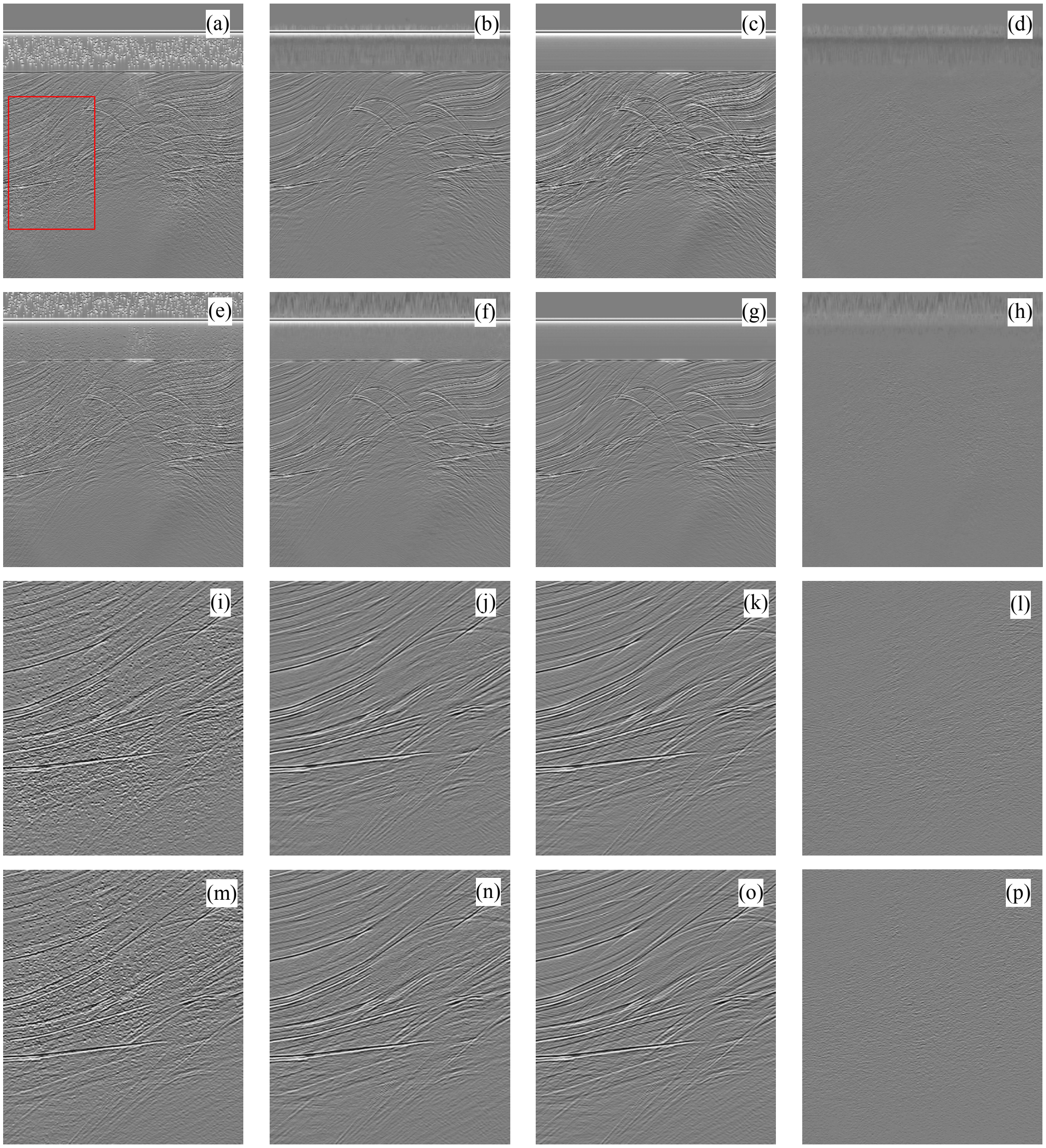

Figure 4: Comparison of the reconstructed deblended data and the unblended data: (a) Blended primary common offset gather, (b) Reconstructed primary source, (c) True unblended primary source, (d) Difference between reconstructed and unblended primary sources, (e) Blended secondary common offset gather, (f) Reconstructed secondary source, (g) True unblended secondary source, (h) Difference between reconstructed and unblended secondary sources, (i) Zoomed-in details of blended primary common offset gather in the area maeked in Figure 4a, (j) Zoomed-in details of reconstructed primary source, (k) Zoomed-in details of true unblended primary source, (l) Zoomed-in details of the difference between reconstructed and unblended primary sources, (m) Zoomed-in details of blended secondary common offset gather, (n) Zoomed-in details of reconstructed secondary source, (o) Zoomed-in details of true unblended secondary source, and (p) Zoomed-in details of difference between reconstructed and unblended secondary sources,

DOI http://dx.doi.org/10.1190/segam2014-1510.1

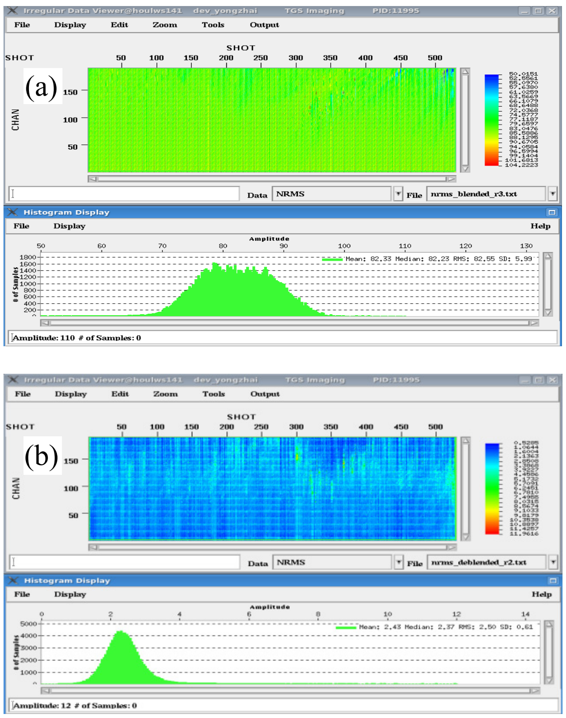

Figure 5: Comparison of the changes to NRMS (normalized RMS) for simultaneous data and unblended data a) Before deblending, and b) After deblending.

The minor difference between the reconstructed and unblended data (Figures 4d and 4h) confirms our data separation and reconstruction job flow works effectively. Figure 5 shows the NRMS between the simultaneous and unblended data has dramatically dropped from an average of 82.3 to 2.4 after 10 iterations. The migration images in Figure 6 also demonstrates that the enhanced adaptive subtraction approach removed most of the artifacts of crosstalk from the simultaneous acquisition, which we cannot attenuate by migration and stack alone especially in the shallow sections.

Conclusions

We developed an enhanced adaptive subtraction method to separate simultaneous data and reconstruct the deblended primary and secondary shot data simultaneously by iteration. This method is an improvement over the TGS legacy processing flow used to separate simultaneous OBC data when the simultaneous sources apart from each other by a certain large distance. The synthetic data test shows our new approach is applicable to streamer data as well, and the simultaneous sources can be close to each other in distance. The reconstructed deblending data and the migration images demonstrate this new technique is quite effective even for relatively weak events and complex structures.

Acknowledgments

The authors appreciate the helpful discussion with Henrik Roende, Will Whiteside, Manhong Guo, James Sheng, Satyakee Sen and Neil Hokanson, and the synthetic data generation by Jian Mao. We also thank Connie VanSchuyver for reviewing the manuscript and the TGS management for permission to publish this work.

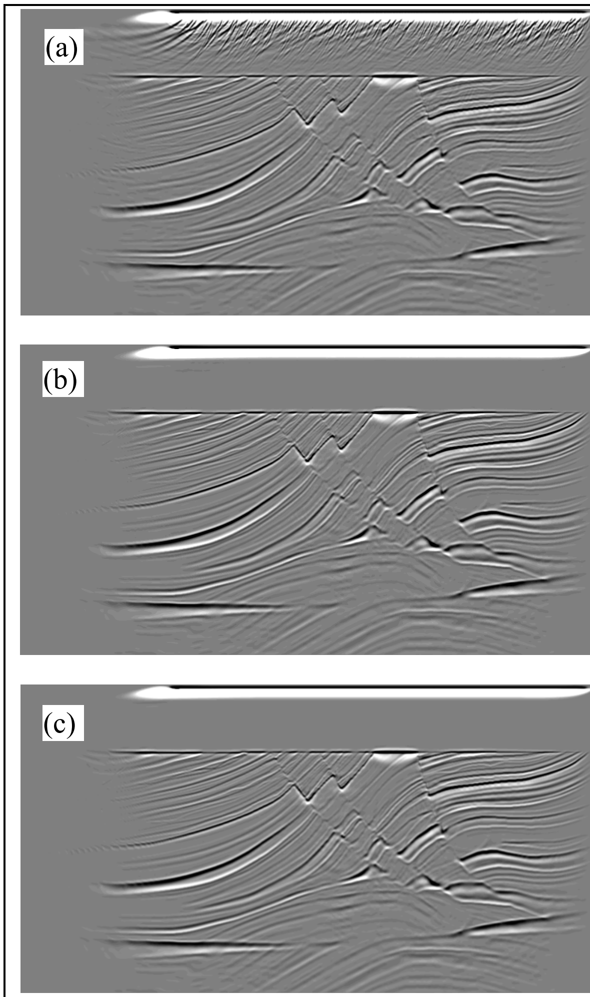

Figure 6: Comparison of the migration images of a) blended data; b) deblended data and c) unblended data.

DOI http://dx.doi.org/10.1190/segam2014-1510.1

http://dx.doi.org/10.1190/segam2014-1510.1

EDITED REFERENCES

Note: This reference list is a copy-edited version of the reference list submitted by the author. Reference lists for the 2014 SEG Technical Program Expanded Abstracts have been copy edited so that references provided with the online metadata for each paper will achieve a high degree of linking to cited sources that appear on the Web.

REFERENCES

Abma, R. L., T. Manning, M. Tanis, J. Yu, and M. Foster, 2010, High-quality separation of simultaneous sources by sparse inversion: 72nd Annual International Conference and Exhibition, EAGE, Expanded Abstracts, B003

Beasley, C. J., R. E. Chambers, and Z. Jiang, 1998, A new look at simultaneous source: 68th Annual International Meeting, SEG, Expanded Abstracts, 133–135.

Huo, S., Y. Luo, and P. G. Kelamis, 2012, Simultaneous sources separation via multidirectional vector-median filtering: Geophysics, **77**, no. 4, V123–V131, http://dx.doi.org/10.1190/geo2011-0254.1.

Kim, Y., I. Gruzinov, M. Guo, and S. Sen, 2009, Source separation of simultaneous source OBC data: 79th Annual International Meeting, SEG, Expanded Abstracts, 51–55.

Mahdad, A., P. Doulgeris, and G. Blacquiere, 2011, Separation of blended data by iterative estimation and subtraction of blending interference noise: Geophysics, **76**, no. 3, Q9–Q17, http://dx.doi.org/10.1190/1.3556597.

Moore, I., W. Dragoset, T. Ommundsen, D. Wilson, C. Ward, and D. Eke, 2008, Simultaneous source separation using dithered sources: 78th Annual International Meeting, SEG, Expanded Abstracts, 2806–2809.

Peng, C., B. Liu, A. Khalil, and G. Poole, 2013, Deblending of simulated simultaneous sources using an iterative approach: An experiment with variable-depth streamer data: 83rd Annual International meeting, SEG, Expanded Abstracts, 4278–4282.